Isolated Airfoil—Tip Vortex Interaction Noise

Robert W. Paterson* and Roy K. Amiet†
United Aircraft Research Laboratories, East Hartford, Conn.
and
C. Lee Munch‡
Sikorsky Aircraft Division, Stratford, Conn.

An experimental investigation was conducted in the UARL Acoustic Research Tunnel to define the noise characteristics associated with the interaction of a stationary tip vortex and a downstream stationary airfoil. This model test geometry simulated, in its simplest form, the tip vortex-blade interaction which occurs on single rotor helicopters during hover. For moderate to high lift test conditions, the vortex-airfoil interaction was found to cause local blade stall with an attendant increase in the blade far-field noise. These results indicated that this interaction may be an important source of helicopter broadband noise during hover. Cross-correlation measurements conducted amongst surface-mounted and far-field microphones demonstrated that the operative noise mechanism was "trailing edge noise" arising from the interaction of stall generated eddies with the airfoil trailing edge. This mechanism would be expected to be responsible for increased noise at stall conditions in other, nonrotary wing, applications.

Nomenclature

c = downstream airfoil chord
c_o = speed of sound
f = frequency
$f(t)$ = surface microphone signal
$g_s(t)$ = filtered surface microphone signal
$g_f(t)$ = filtered far-field microphone signal
h = filter impulse response function
r = trailing edge to far-field microphone separation
C_D = local rotor blade drag coefficient
C_T = rotor thrust coefficient
L = surface microphone to trailing edge separation
M_T = rotor tip Mach number
R_{ff} = autocorrelation of far-field noise
R_{sf} = cross-correlation function between surface and far-field microphones
S = vortex-airfoil vertical separation
St = Strouhal number $= fc/V$
U_c = eddy convection velocity
V = tunnel speed
α_D = downstream airfoil angle of attack
α_u = upstream airfoil angle of attack
ξ = dummy variable
ρ = normalized cross-correlation function amplitude
θ = far-field noise directivity angle
σ = rotor solidity
τ = delay time
ζ = position of 30% chord microphone

Introduction

A PREVIOUSLY unexplored but potentially important source of helicopter broadband noise during hover is the interaction of a rotor blade tip vortex with the following blade. Previous studies[1-3] have been concerned with the blade slap problem in which the interaction of a moving blade with a tip vortex shed from another blade produces harmonic noise. The present study was directed toward the temporally steady problem of the interaction of a stationary vortex and airfoil. This configuration is relevant to a hovering helicopter where the trajectory of a blade tip vortex is downward and radially inward causing the vortex to pass beneath the following blade in the vicinity of the tip. In an idealized model of this phenomenon the blade tip vortex strengths can be considered constant with time and the vortex trajectories fixed relative to the blades. Viewed from a rotor fixed coordinate system the noise generation process in this model consists of the interaction of the potential field of a stationary tip vortex and a downstream stationary airfoil. The purpose of the study reported here was to experimentally determine the noise characteristics associated with this interaction in an acoustic wind tunnel at Mach numbers approaching full scale and with vortex-blade parameters scaled from typical rotor operating conditions.

Experimental Arrangement

This study was conducted in the United Aircraft Research Laboratories Acoustic Research Tunnel. The tunnel, shown schematically in Fig. 1 and described in detail elsewhere,[4] is a controlled turbulence level, open-jet wind tunnel designed specifically for aerodynamic noise research. For the present study, the total turbulence level in the test section was 0.2%. Far-field noise measurements were carried out in the quiescent region approximately 6 ft above the test section centerline in the sealed anechoic chamber which surrounded the test section. This chamber has been determined to be anechoic for broadband noise above 200 Hz.[4]

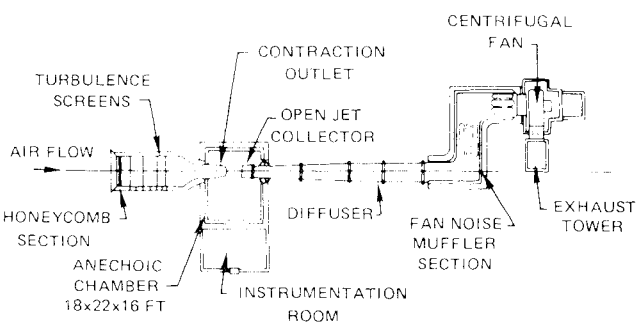

Fig. 1 UARL acoustic research tunnel.

Presented as Paper 74-194 at the AIAA 12th Aerospace Sciences Meeting, Washington, D.C., January 30–February 1, 1974; submitted February 2, 1974; revision received July 31, 1974. The experimental study reported herein was funded by the Army Research Office, Durham, under Contract DAHC04-72-C-0040. The authors wish to acknowledge helpful discussions with H. P. Day (UARL), A. A. Peracchio (Pratt and Whitney Aircraft), and D. R. Clark (Sikorsky Aircraft).

Index category: Aircraft Noise, Aerodynamics (Including Sonic Boom).

*Supervisor, Aeroacoustics Group, United Aircraft Research Laboratories. Member AIAA.

†Senior Research Engineer, Aeroacoustics Group, United Aircraft Research Laboratories.

‡Supervisor, Acoustics Group, Sikorsky Aircraft.

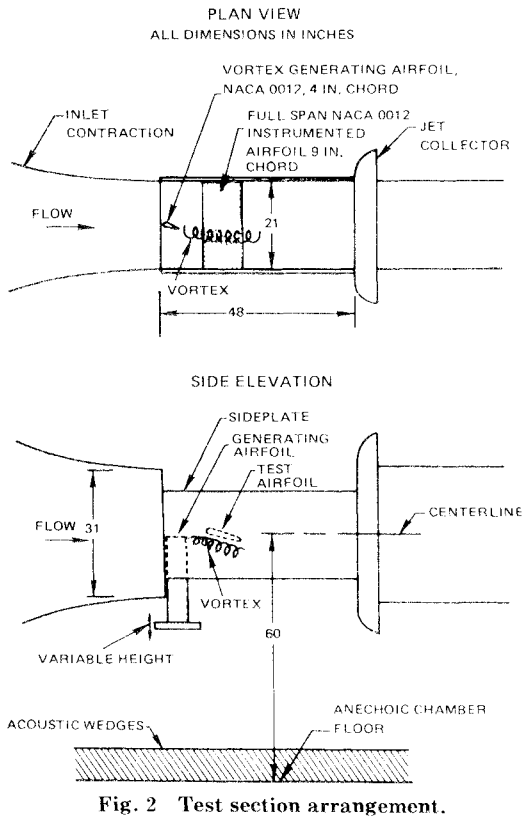

Fig. 2 Test section arrangement.

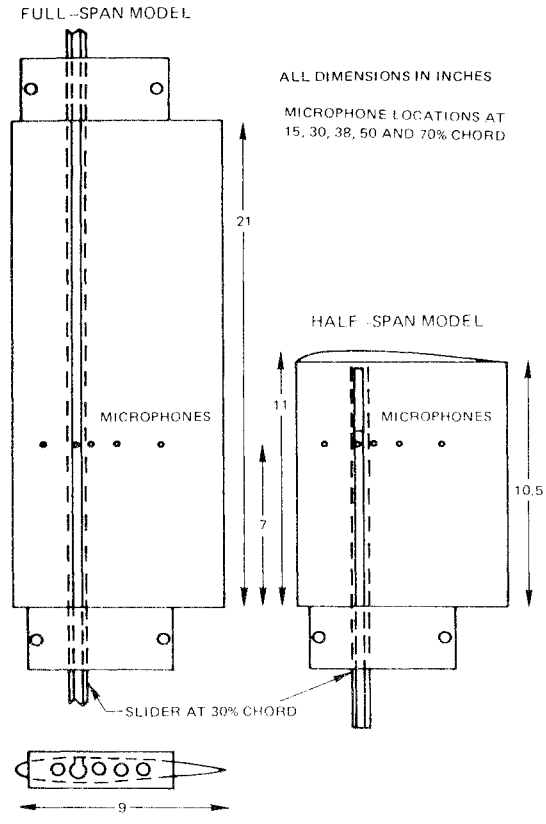

Fig. 3 NACA 0012 airfoil models.

Figure 2 shows the test section arrangement employed in this study. A tip vortex was generated by a 4 in. chord, NACA 0012 airfoil oriented vertically. This vortex convected downstream and passed beneath a 9 in. chord, NACA 0012 instrumented airfoil, which was oriented horizontally and spanned the test section. The relative perpendicular orientation of the airfoils permitted the vortex interaction mechanism to be studied in the absence of noise caused by impingement of the upstream airfoil wake on the downstream airfoil. In addition, this arrangement most accurately simulated the helicopter vortex-blade encounter. The tip vortex strength and position were varied by varying the upstream airfoil angle of attack and vertical position, respectively. To obtain a uniform spanwise loading on the full-span airfoil model, the vertical sides of the jet were closed with sideplates extending from the wind tunnel contraction outlet into the jet collector. The full-span model was instrumented with an array of four fixed and one movable ¼ in. diam flush-mounted condenser microphones on the airfoil suction surface, as shown in Fig. 3, to permit measurement of the local fluctuating surface pressure in both the span and chord directions. The microphone protective grids were removed and the diaphragms optically aligned with the airfoil surface to minimize the potential disturbance of surface microphone measurements by wakes from upstream microphones. Tests demonstrated that the 30% and 38% chord surface pressure spectra did not change when the 30% chord microphone was moved from a position directly downstream from the 15% chord microphone to a position offset in span. From this it was concluded that the surface microphones produced no mutual interference. In addition to the full-span airfoil, Fig. 3 shows an instrumented half-span model which was tested to evaluate vortex interaction noise due to tip region encounters.

All listed angles of attack are geometric angles which require a negative correction[5] to compensate for two-dimensional open jet wind tunnel effects. Frequency spectrum and correlation analyses were conducted on-line during testing employing both a real time spectrum analyzer-ensemble averager and real time correlation and probability analyzer.

Experimental Results

Summary

It was generally observed that the passage of the tip vortex beneath the test airfoil had a measurable effect on the unsteady surface pressures and the far-field noise for only those test conditions in which the tip vortex caused local blade stall to occur (as indicated by tufts). For the conditions tested, it was also observed that the far-field noise was independent of vortex strength and position as independent variables, depending only on sufficient induced upwash to cause downstream airfoil stall. The far-field noise power spectral density at constant Strouhal number was tentatively found to vary with velocity to the fourth power for the low frequencies which dominated the spectra. The following sections discuss the experimental results in greater detail in terms of surface pressure, far-field noise and correlation function measurements.

Surface Pressure Measurements

Figure 4 displays typical surface pressure spectra obtained with and without an upstream generated tip vortex at test conditions scaled to represent high rotor thrust. The data were obtained with the downstream airfoil at an angle of attack, α_D = 13.5°, and with a tunnel speed, V = 450 fps (Reynolds number = 2.2 × 10^6). The vertical separation of the tip vortex and the downstream airfoil pressure surface at ¼ chord, S, was assumed to be approximately 1 in. (based on a measurement of the vortex position at 100 fps). The tip vortex generated by the upstream airfoil at an angle of attack, α_U = 8°, caused the 30 and 70% chord fluctuating surface pressures to increase on the order of 20 to 30 db at low frequencies with smaller increases obtained at high frequencies. These large increases

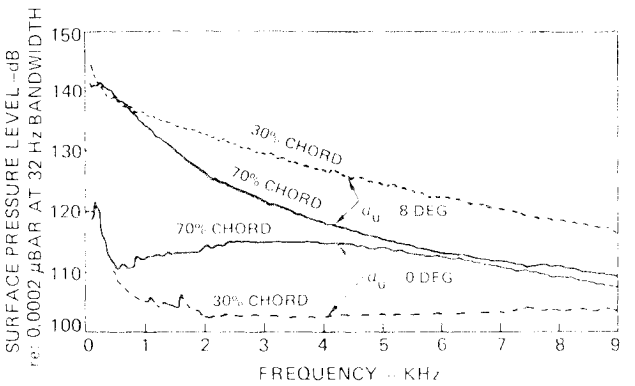

Fig. 4 Effect of tip vortex interaction on 30% and 70% chord unsteady surface pressure, V = 450 fps, α_{lf} = 13.5°, α_u = 0° and 8°, $S \approx 1$ in., NACA 0012 full span airfoil.

were associated with airfoil leading-edge-stall as confirmed by flow visualization with tufts. Increases of these magnitudes, which were also observed at the other instrumented locations between 15% and 70% chord, would be expected to cause a significant increase in the radiated noise. Whereas both microphone locations in Fig. 4 record similar low-frequency amplitudes, the high frequency amplitudes were significantly higher at the forward location when the flow was stalled. The opposite behavior is observed with attached turbulent boundary layers on airfoils as shown in Fig. 4 by the α_u = 0 deg curves and in more detail elsewhere.[6]

The results of a spanwise survey for the same operating condition are given in Fig. 5. The upper portion of the figure shows the orientation and position of the upstream vortex relative to the spanwise survey locations of the 30% microphone which was capable of traversing spanwise.

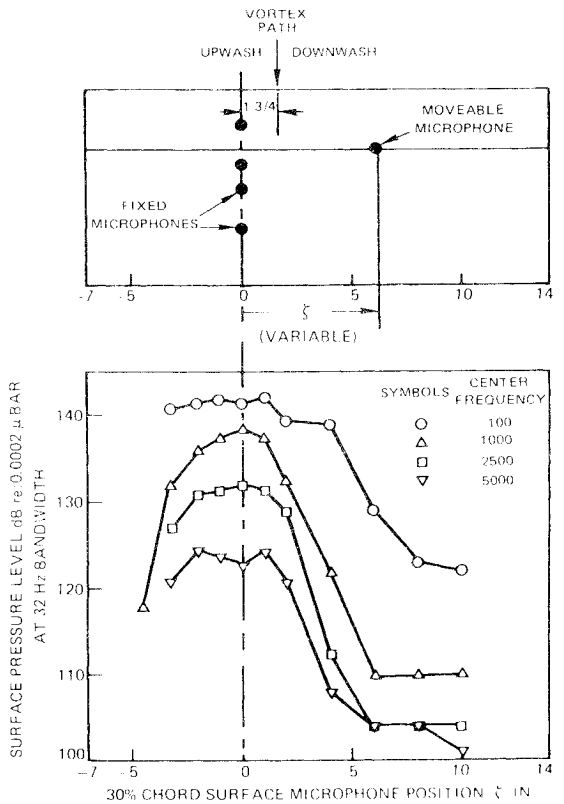

Fig. 5 Effect of tip vortex interaction on spanwise distribution of unsteady surface pressure, V = 450 fps, α_{lf} = 13.5°, α_u = 8°, $S \approx 1$ in., NACA 0012 full span airfoil.

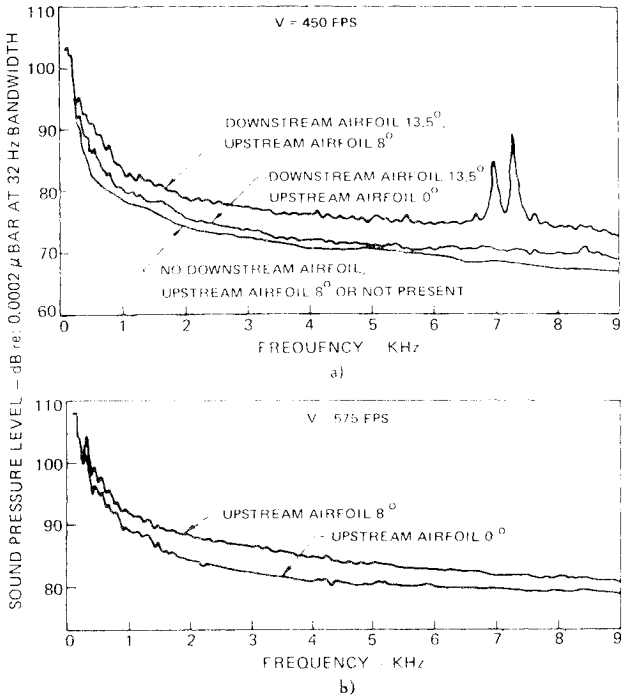

Fig. 6 Effect of tip vortex interaction on far-field noise for two velocities, α_{lf} = 13.5°, α_u = 8°, $S \approx 1$ in., NACA 0012 full span airfoil.

The lower plot presents the pressure fluctuation amplitudes as a function of frequency. The large increases in pressure level at 1000 Hz relative to 5000 Hz in the vicinity of the vortex path (ζ = 1.75 in.) confirm the results of Fig. 4 that the stall phenomena is dominated by low frequency fluctuations. From the 1000 Hz data given in Fig. 5, the spanwise extent of the stall region can be estimated to be approximately 10 in. (in general agreement with flow visualization tuft results). The stall region extends partially into the region of span experiencing downwash (ζ > 1.75 in.) although surface pressure fluctuations were largest in the region where the vortex produced upwash and hence increased local incidence. For large ζ, the unsteady pressure decreased to the unsteady pressure level typical of the unstalled airfoil.

For vortex strengths, vertical positions, and downstream airfoil angles of attack such that stall did not occur, the passage of the tip vortex under the downstream airfoil had no measurable effect on the unsteady surface pressure; hence, no effect would be expected in the far field.

Far-Field Noise Measurements

Prior to considering the far-field microphone measurements, it should be noted that the occurrence of stall was plainly audible to observers in the chamber. As the upstream airfoil was rotated to produce increasing vortex strength, an angle of attack would be reached which caused a sudden increase in noise and simultaneously, stalled airfoil flow as indicated by tufts.§ The stall noise was qualitatively of a buffeting low-frequency nature.

Figure 6a presents the effect of the tip vortex interaction on the far-field noise 6 ft above the test section centerline at the test condition considered above. The lowest curve, corresponding to a test configuration of no downstream airfoil and the upstream airfoil at 8°, was essentially a measurement of the empty tunnel background noise (noise due to the turbulent open jet shear layer and

§Tests conducted without tufts produced the same far-field noise.

its impingement on the downstream collector) since the presence of the upstream airfoil caused no measurable increase in noise over tunnel-empty conditions. The next higher spectrum was obtained with the upstream airfoil at 0° (no tip vortex) and the downstream airfoil at 13½°. Due to open jet wind tunnel effects,[5] the airfoil was unstalled at this high angle of attack. There is experimental evidence[4] to support the conclusion that the increased noise measured in this high lift configuration is not downstream airfoil noise but tunnel background noise arising from distorted inflow into the tunnel open-jet collector. This distortion is caused by deflection of the tunnel open jet by the lifting airfoil. This represents a significant limitation to noise testing, for only strong airfoil noise mechanisms such as vortex shedding[6] stand out above tunnel background.

Based on the preceding measurements, the appropriate background noise for the experiment is the spectrum obtained with the downstream airfoil at 13½° and with the upstream airfoil at zero lift. The highest spectrum in Fig. 6a then shows the increased noise due to the tip vortex induced local blade stall.

The two high-frequency discrete tones at 7000 Hz and 7300 Hz are an indirect result of the tip vortex presence and are not associated with local blade stall. These spikes are due to vortex shedding from the unstalled portion of the blade trailing edge and arose when the tip vortex downwash caused the pressure surface boundary layer at the trailing edge to undergo transition from turbulent to laminar flow (see Fig. 4, Ref. 6). Although the vortex shedding tones are not related to the local stall noise under study, and occurred for only a limited number of test conditions, the relative equal magnitude of the vortex tones and the stall noise (below 1000 Hz) indicates that the two mechanisms will have comparable amplitudes although the former is a high-frequency discrete tone phenomenon and the latter is a low-frequency broadband phenomenon. Since vortex tone noise has been shown to dominate the noise spectra of full-scale rotors when the mechanism occurs (e.g., Fig. 12, Ref. 6), the above argument suggests that tip vortex interaction noise would be expected to dominate the low-frequency rotor noise when local blade stall occurs.

From Fig. 6a it is evident that vortex-induced local blade stall caused a measurable increase in the noise above tunnel background noise for frequencies above 250 Hz. It is clear that the radiated noise was broadband with the dominant frequencies in the stall noise spectrum occurring below 1000 Hz, in agreement with the measured surface pressure spectra. The importance of the stall noise mechanism is obscured to some extent by the fact that the background noise measurement was not one of airfoil noise in the absence of a tip vortex but one dominated by the wind tunnel open jet collector noise.

Figure 6b presents vortex interaction and background noise spectra at a higher tunnel speed of 575 fps, a value approaching typical full scale rotor tip velocities. The interaction noise, again due to blade stall, is observed to stand out some 2 to 4 db above background for frequencies above 500 Hz. Background noise spectra have been included in these figures rather than subtracted from the interaction noise spectra to permit assessment of the experimental signal to noise ratio. These spectra tend to overestimate the background noise since stalled airfoil flow produces less jet deflection, and hence collector noise, than unstalled flow at the same downstream airfoil angle of attack. Far-field noise measurements conducted over the velocity range from 100 to 650 fps invariably showed an increase above tunnel background when local stall occurred. The small signal-to-noise ratio, however, precluded precise determination of the dependence of stall noise spectra on velocity. For amplitude comparisons carried out at constant Strouhal number, St, the far-field sound pressure level at constant bandwidth analysis measured directly above the airfoil was found to vary approximately with velocity to the 4th power for low Strouhal numbers (on the order of 1) which dominate the spectra, increasing to a higher power dependence with increasing Strouhal number.

Once local blade stall was observed to occur, for the conditions tested, further increases in vortex strength or downstream airfoil angle of attack failed to produce either a further increase in the far-field noise or an increase in the spanwise extent of stall. This noise generation process therefore appears to depend primarily on the existence of stall while being insensitive to the individual parameters which either cause or tend to aggravate the stalled condition. Measurements conducted with the half-span NACA 0012 model produced interaction noise spectra similar to those of the full-span model with the exception that higher geometric angles of attack were required to produce stall. This can be attributed to the decrease in effective angle of attack caused by the tip vortex of the downstream half-span airfoil.

Identification of Noise Production Mechanism

A series of cross-correlation measurements were conducted at test conditions for which vortex induced stall occurred on the downstream blade in order to further define the characteristics of the noise production process. Correlations conducted amongst surface microphones arrayed in the chordwise direction indicated the presence of downstream convected eddies with a convection velocity approximately equal to 0.3 times the freestream velocity V. Cross-correlations conducted between the far-field microphone and the surface microphones, however, indicated that these eddies were not directly radiating noise to the far field.

The use of longitudinal space-time cross-correlations among surface transducers to determine eddy convection velocities as reported here is a well-established technique described in detail elsewhere.[7] In addition to these surface-surface cross-correlations, cross-correlations were conducted between the far-field microphone and surface microphones arrayed in the chordwise direction. This use of this technique to obtain quantitative information regarding local acoustic source strengths on surfaces is described in detail elsewhere.[8]

Cross-correlations conducted between the far-field microphone and the surface microphones indicated that the

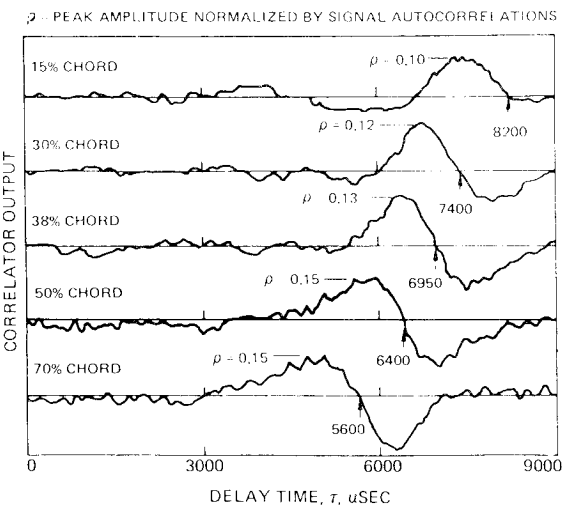

Fig. 7 Cross-correlation functions between far-field and surface microphones for five surface microphone chordwise positions, V = 450 fps, α_D = 13.5°, α_u = 8°, S = 1 in., NACA 0012 full span airfoil.

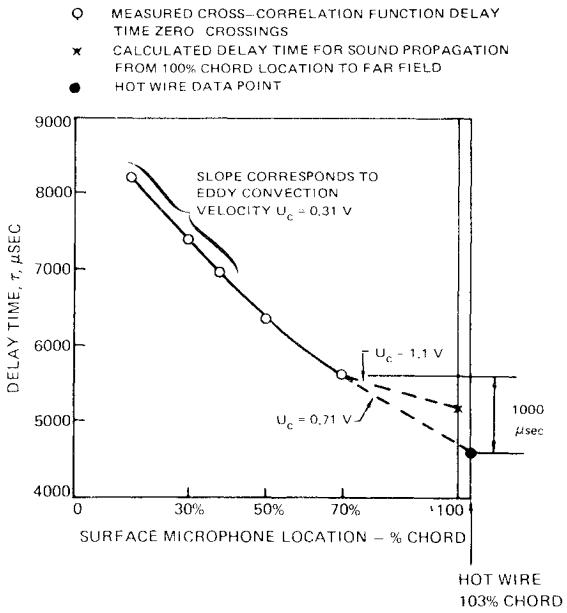

Fig. 8 Far-field and surface cross-correlation zero-crossings replotted from Fig. 7. Hot wire—70% chord surface microphone cross-correlation also shown for same test condition.

eddies measured during surface-surface microphone correlations were not directly radiating noise to the far field. This is evident from Fig. 7 which presents surface-far-field cross-correlation functions at a typical test condition [same condition as Figs. 4, 5, and 6(a)] for each of the five chordwise surface microphones. In this figure, positive delay time corresponds to delay of the surface microphone signal with respect to the far-field microphone signal. Both signals were filtered prior to correlation by a 250 Hz high pass filter to eliminate low frequency noise associated with the tunnel fan. As discussed in the following section, the zero-crossing time delay centered on the peak correlation region of the functions (indicated by an arrow) represents the time required for the disturbance measured by the surface microphone to manifest itself as noise in the far field. For all surface microphone positions this time delay was considerably in excess of the acoustic propagation time of approximately 5250 μsec. (This value includes, in addition to the acoustic propagation time, a calculated additional delay of 100 μsec associated with a lengthening of the sound propagation path by refraction in the tunnel open jet shear layer.) The monotonic decrease in the zero-crossing time delay value with increasing chord indicates that the eddies propagated downstream but produced significant noise only when they approached the airfoil trailing edge.

The previous zero-crossing time delays are replotted in Fig. 8 as a function of microphone chordwise position. The slope of the upper portion of the curve corresponds to an eddy convection velocity of 0.31 times the freestream velocity, a value in agreement with the surface-surface cross-correlation results discussed above. The convection velocity is observed to increase with chord as indicated by the decreasing slope of the curve. The slope of the curve between the 70% chord data point and the 100% chord delay time marked by an "x" (corresponding to propagation from 100% chord to the far field) in Fig. 8, however, would require the improbably high convection velocity of 1.1 *V*. This suggests that the noise production process occurs somewhat upstream from the trailing edge.

To more fully explore this mechanism, a crossed hot-wire probe was placed ¼ in. downstream of the airfoil trailing edge and at the same spanwise position as the surface microphones, to measure the vertical component of the fluctuating velocity. Cross-correlation between the 70% chord surface microphone and the hot wire showed a peak correlation at 1000 μsec implying a local eddy convection velocity of 0.71 *V*. This result appears to confirm the above conclusion that the local convection velocity does not exceed the freestream value and that the source of noise is therefore somewhat upstream of the edge. This result appears reasonable in light of the Kutta condition, which by requiring zero pressure differential between the upper and lower airfoil surfaces precludes the presence of a dipole exactly at the trailing edge.

Interpretation of Surface-Far Field Cross-Correlation Time Delays

To interpret surface pressure-far field noise cross-correlation measurements as applied to edge noise, it is useful to first consider the noise production process of a surface with no bounding edge, that of a turbulent boundary layer on an infinite flat plate. If the fluctuating viscous stresses parallel to the surface are assumed to be small, one is left with a normal force produced by the fluctuating surface pressure. As was discussed by Powell[9] among others, this distribution of surface forces leads to a quadrupole type of noise rather than the more efficient dipole noise. This obtains since the boundary condition of no flow through the plate can be satisfied by imposing a mirror image boundary layer below the plate and then removing the plate. Thus, for an infinite flat plate, the original boundary layer and its mirror image produce only quadrupole sound which is an inefficient source when compared to a dipole.

If instead of an infinite plate we consider a finite plate, the mirror image argument employed above no longer applies for an eddy near the edge. As discussed by Ffowcs Williams and Hall[10] and Hayden,[11] under certain conditions the noise produced by the surface forces in the vicinity of the edge can significantly outweigh the ordinary type of boundary-layer noise previously discussed. Ffowcs Williams and Hall[10] predict the edge noise mechanism to cause the over-all noise level to vary as velocity to the 5th power while over-all boundary-layer noise behaves as velocity to the 8th. Thus, if one considers the case of an eddy moving downstream toward an edge at moderate subsonic velocities, the sound production will be small when the eddy is far upstream of the edge. As the eddy progresses downstream, fluctuating dipole forces will be produced in the vicinity of the edge. The upstream plate acts as a baffle which alters the directivity from a dipole pattern (behaving as $\sin\theta$) to a $\sin\theta/2$ behavior where θ is measured forward from the plate trailing edge.

The previous argument suggests that a pressure transducer on the surface of the plate would sense a disturbance when an eddy convected past it, but little sound would be generated until the eddy reached the vicinity of the trailing edge. If on reaching the trailing edge the eddy had not changed its characteristics significantly, a cross-correlation between a surface and far-field microphone would be expected to show a peak at approximately the delay time, τ_0, equal to the sum of the time required for the eddy to convect downstream from the surface microphone to the trailing edge region and that required for sound to propagate from the edge to the far-field microphone. As mentioned in the preceding section, this was observed in the present study.

In this experiment the microphone signals were filtered before being cross-correlated. This results in a sine wave of variable amplitude with an envelope peak in the vicinity of the above mentioned delay time, τ_0. In order to define the delay time more precisely, the zero-crossing point occurring between the two largest peaks was used for determining the time delay between the appearance of a signal on the surface microphone and the measurement of the far-field sound. Some justification for this procedure

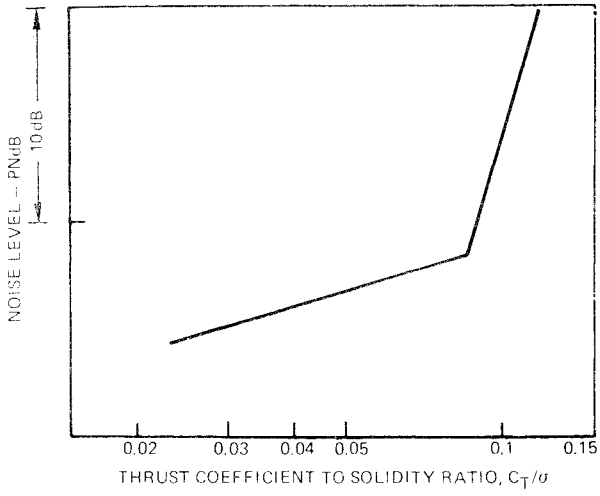

Fig. 9 Trend of single rotor helicopter perceived noise level with increasing thrust showing noise divergence.

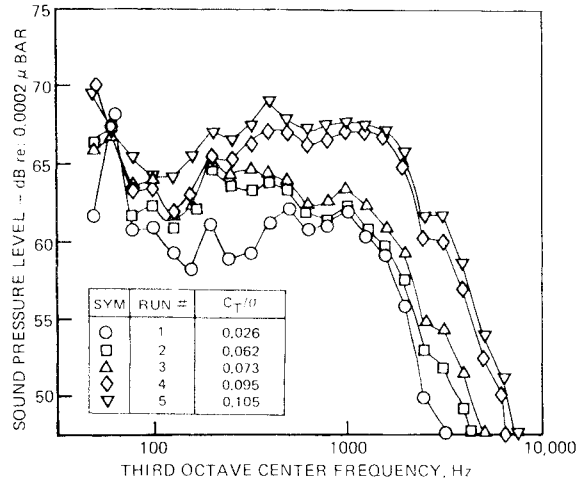

Fig. 10 Full-scale rotor third-octave spectra as a function of thrust showing noise divergence, $M_T = 0.56$ (from unpublished results).

can be given: assuming that the far-field sound is produced at the trailing edge and that a surface microphone measures a signal $f(t)$, then the fluctuating surface pressure near the trailing edge (and also the lift) would be expected to be proportional to $f(t - L/U_c)$ where L is the distance between the surface microphone and the trailing edge, and U_c is the eddy convection velocity. Since the far-field microphone is located directly above the airfoil (the retarded time is constant for all points on the airfoil), the far-field sound would be proportional to the time derivative of the lift or $\dot{f}(t - L/U_c)$[12]. If $g_s(t)$ and $g_f(t)$ represent the filtered surface and far-field signals, respectively, then:

$$g_s(t) = \int_{-\infty}^{+\infty} f(t - \xi)h(\xi)d\xi \tag{1}$$

$$g_f(t) = \int_{-\infty}^{+\infty} \dot{f}\left(t - \xi - \frac{r}{c_o} - \frac{L}{U_c}\right)h(\xi)d\xi \tag{2}$$

where $h(\xi)$ represents the filter impulse response function, r the distance between the trailing edge and the far field, and c_o the speed of sound. The cross-correlation $R_{sf}(\tau)$ between g_s and g_f is then related to the autocorrelation of the far-field signal, $R_{ff}(\tau)$ as follows:

$$R_{sf}(\tau) = \lim_{T\to\infty} \frac{1}{2T} \int_{-T}^{+T} \int_{-\infty}^{+\infty} \int_{-\infty}^{+\infty} h(\xi_1)h(\xi_2)f(t - \xi_1)\dot{f}$$
$$\left(t + \tau - \xi_2 - \frac{r}{c_o} - \frac{L}{U_c}\right)dtd\xi_1d\xi_2 = \frac{\partial}{\partial\tau}\int_{-\infty}^{+\infty}\int_{-\infty}^{+\infty} R_{ff}$$
$$\left(\tau - \frac{r}{c_o} - \frac{L}{U_c} + \xi_1 - \xi_2\right)h(\xi_1)h(\xi_2)d\xi_1d\xi_2 \tag{3}$$

Since the double integral is symmetric about $\tau = (r/c_o) + (L/U_c)$, the derivative with respect to τ is zero for $\tau = (r/c_o) + (L/U_c)$; i.e., $R_{sf}(\tau = r/c_o + L/U_c) = 0$. Thus, the surface far-field cross-correlation would be expected to have a zero crossing at the retarded time $\tau = (r/c_o) + (L/U_c)$ which should also be near the maximum of the envelope which contains the variable amplitude sinusoidal wave.

Relationship of Results to Full-Scale Rotor Noise

The primary results of the present study have been to identify blade local stall noise as a source of broadband noise on a model scale and to determine the detailed mechanism responsible for such noise. Since helicopter rotors operating at high thrust are known to produce similar local stall pockets, an increase in rotor broadband noise would be expected at the onset of stall. Further experimentation (for example, to determine the stall noise directivity pattern) will be required before the importance of this mechanism can be fully assessed relative to other rotor broadband noise mechanisms. The following brief discussion of rotor noise, however, suggests that the stall mechanism may account for a previously unexplained rotor noise phenomenon.

Classically, it is expected that rotor system noise should increase uniformly with increasing thrust. Recent noise measurements conducted on full-scale helicopter rotor systems have confirmed this trend for low values of the ratio of thrust coefficient to solidity (C_T/σ). As shown schematically in Fig. 9 and in more detail in Fig. 10 (from unpublished full-scale results), however, C_T/σ values in the range from 0.08 to 0.09 (rotor tip Mach number $M_T = 0.56$) cause the noise to "diverge" and increase at a more rapid rate with further increases in this parameter. This behavior has been observed on several different rotor systems and is referred to as "noise divergence."

Figure 10 presents third-octave spectra as a function of thrust for a full scale main rotor operating in hover at a tip Mach number of 0.56. A large increase in the noise

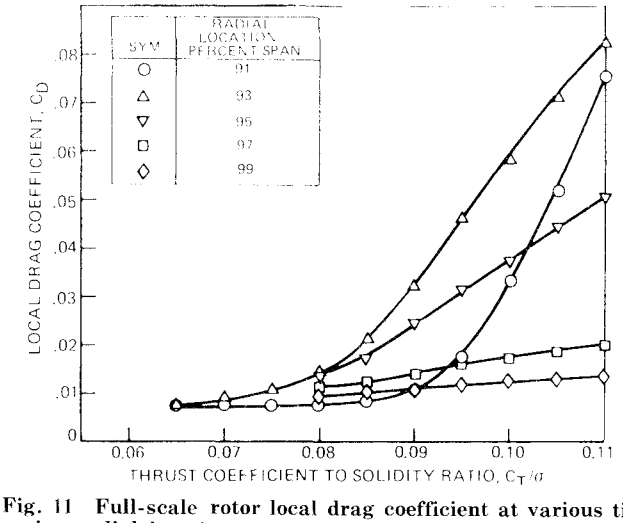

Fig. 11 Full-scale rotor local drag coefficient at various tip region radial locations as a function of thrust (from unpublished results).

level occurs at thrust values above the point of noise divergence (Runs 4 and 5). Analyses conducted at 1.5 Hz bandwidth showed that harmonic noise was undetectable for these thrust values at frequencies greater than about 800 Hz. The large increase in third octave levels at the higher frequencies can therefore be attributed to a broadband noise mechanism.

At C_T/σ values of 0.08 to 0.09, full-scale tests have shown that the local blade drag coefficient, C_D, increases at spanwise positions located above the tip vortex shed from the preceding blade. Figure 11 (from unpublished full-scale results) displays this effect. Movies taken from the rotor hub of a tufted full scale blade operating at design speed confirm that the onset of this drag increase occurs simultaneously with the formation of a local blade stall pocket similar to that studied in the present model test program. The observed concurrent appearance of stall and increased noise on full scale rotors and similar observations in the present experimental study suggest that the tip vortex interaction is the cause of "noise divergence." Rotor test data, however, show a continued increase in noise with thrust above stall which cannot be explained by the model study. The reason for this continued increase is not known.

Vortex passage positions, strengths, and downstream airfoil angles of attack surveyed in this study were chosen to simulate, on a model scale, the encounter between a blade and tip vortex for a 26 in. chord, 36 ft radius, six-bladed main rotor in hover. Vortex induced local blade stall was found to occur in the model tests at a downstream airfoil angle of attack within 2° of that predicted by full-scale data. This is considered good agreement in light of the uncertainties inherent in the scaling and in wind tunnel corrections.

Conclusions

The highly turbulent flow associated with airfoil stall is a source of high-intensity broadband noise. The detailed generating mechanism is the interaction of eddies with the airfoil trailing edge. This noise source arising from vortex interaction appears to explain, at least in part, the phenomenon of helicopter rotor "noise divergence."

References

[1]Surendriah, M., "An Experimental Study of Rotor Blade-Vortex Interaction," CR-1573, May 1970, NASA.

[2]Widnal, S. E., "Helicopter Noise Due to Blade-Vortex Interactions," *Journal of the Acoustical Society of America*, Vol. 50, No. 1, 1971, pp. 354–365.

[3]Filotas, L. T., "Vortex Induced Helicopter Blade Loads and Noise," *Journal of Sound and Vibration*, Vol. 27, No. 3, 1973, pp. 387–398.

[4]Paterson, R. W., Vogt, P. G., and Foley, W. M., "Design and Development of the United Aircraft Research Laboratories Acoustic Research Tunnel," *Journal of Aircraft*, Vol. 10, No. 7, July 1973, pp. 427–433.

[5]Pope, A. and Harper, J. J., *Low Speed Wind Tunnel Testing*, Wiley, New York, 1966, p. 316.

[6]Paterson, R. W., Vogt, P. G., Fink, M. R. and Munch, C. L., "Vortex Noise of Isolated Airfoils," *Journal of Aircraft*, Vol. 10, No. 5, May 1973, pp. 296–302.

[7]Willmarth, W. W. and Wooldridge, C. E., "Measurements of the Fluctuating Pressure at the Wall Beneath a Thick Turbulent Boundary Layer," *Journal of Fluid Mechanics*, Vol. 14, Pt. 2, Oct. 1962, pp. 187–210.

[8]Siddon, T. E., "Surface Dipole Strength by Cross-Correlation Method," *Journal of the Acoustical Society of America*, Vol. 53, No. 2, Feb. 1973, pp. 619–633.

[9]Powell, A., "On the Aerodynamic Noise of a Rigid Flat Plate Moving at Zero Incidence," *Journal of the Acoustical Society of America*, Vol. 31, No. 12, Dec. 1959, pp. 1649–1653.

[10]Ffowcs Williams, J. E. and Hall, L. H., "Aerodynamic Sound Generation by Turbulent Flow in the Vicinity of a Scattering Half Plane," *Journal of Fluid Mechanics*, Vol. 40, Pt. 4, 1970, pp. 657–670.

[11]Hayden, R. E., "Fundamental Aspects of Noise Reduction from Powered-Lift Devices," presented at the Air Transportation Meeting, Society of Automotive Engineers, Miami, Fla., April 24–26, 1973.

[12]Clark, P. J. F. and Ribner, H. S., "Direct Correlation of Fluctuating Lift with Radiated Sound for an Airfoil in Turbulent Flow," *Journal of the Acoustical Society of America*, Vol. 46, No. 3, Pt. 2, 1969, pp. 802–805.